Supplementary Material for

Promotion mechanism of -OH group intercalation for NOx purification on BiOI photocatalyst

Weiping Yang[a], Qin Ren[a], Fengyi Zhong[a], Yanxia Wang[a], Jielin Wang[a], Ruimin Chen[a], Jieyuan Li[a, b*], Fan Dong[a, b]

a. Research Center for Environmental and Energy Catalysis, Institute of Fundamental and Frontier Sciences, University of Electronic Science and Technology of China, Chengdu 611731, China.

b. Yangtze Delta Region Institute (Huzhou), University of Electronic Science and Technology of China, Huzhou, 313000 China.

*Corresponding Author

Jieyuan Li (jieyli@uestc.edu.cn)

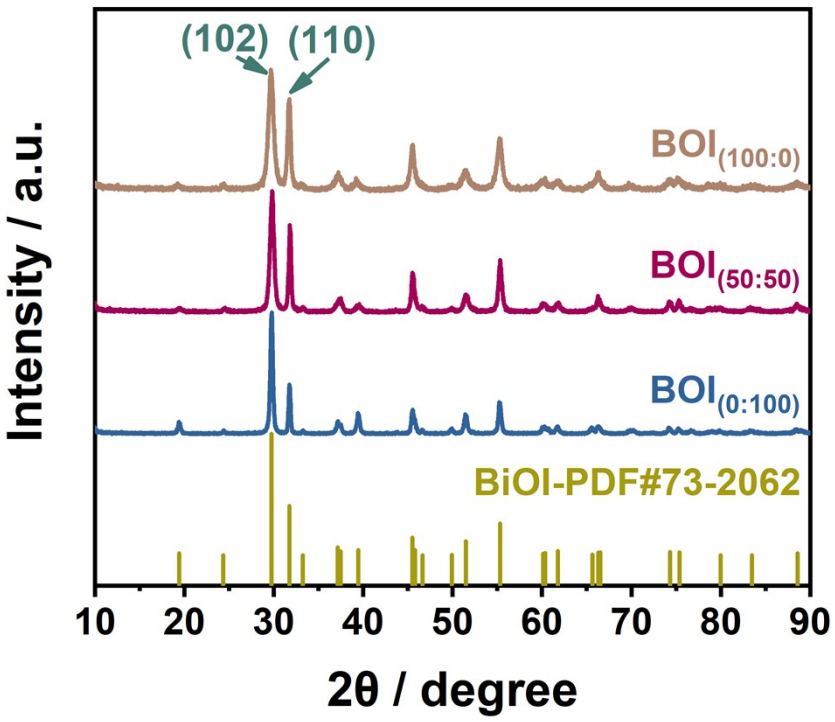

Figure S1. Whole XRD patterns of the photocatalytic materials.

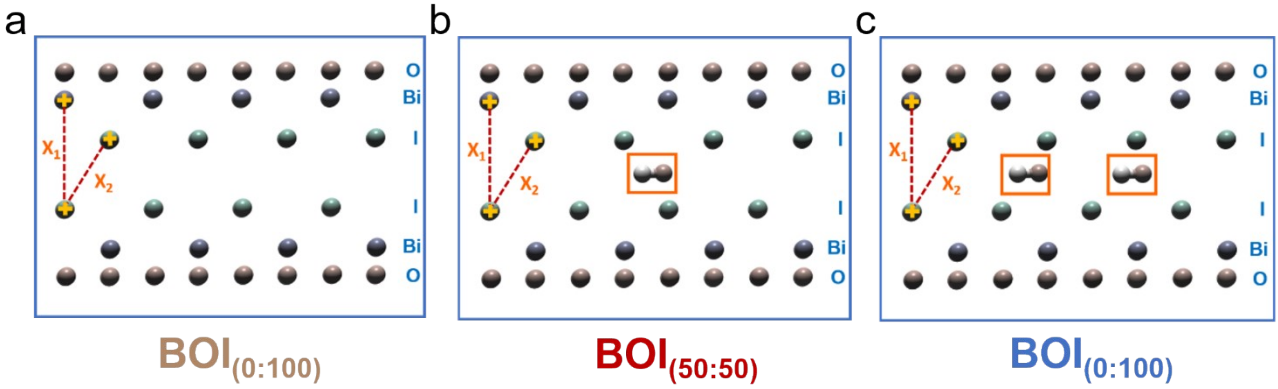

Figure S2. Structure cell with DFT calculation of $BOI_{(0:100)}$, $BOI_{(50:50)}$ and $BOI_{(100:0)}$.

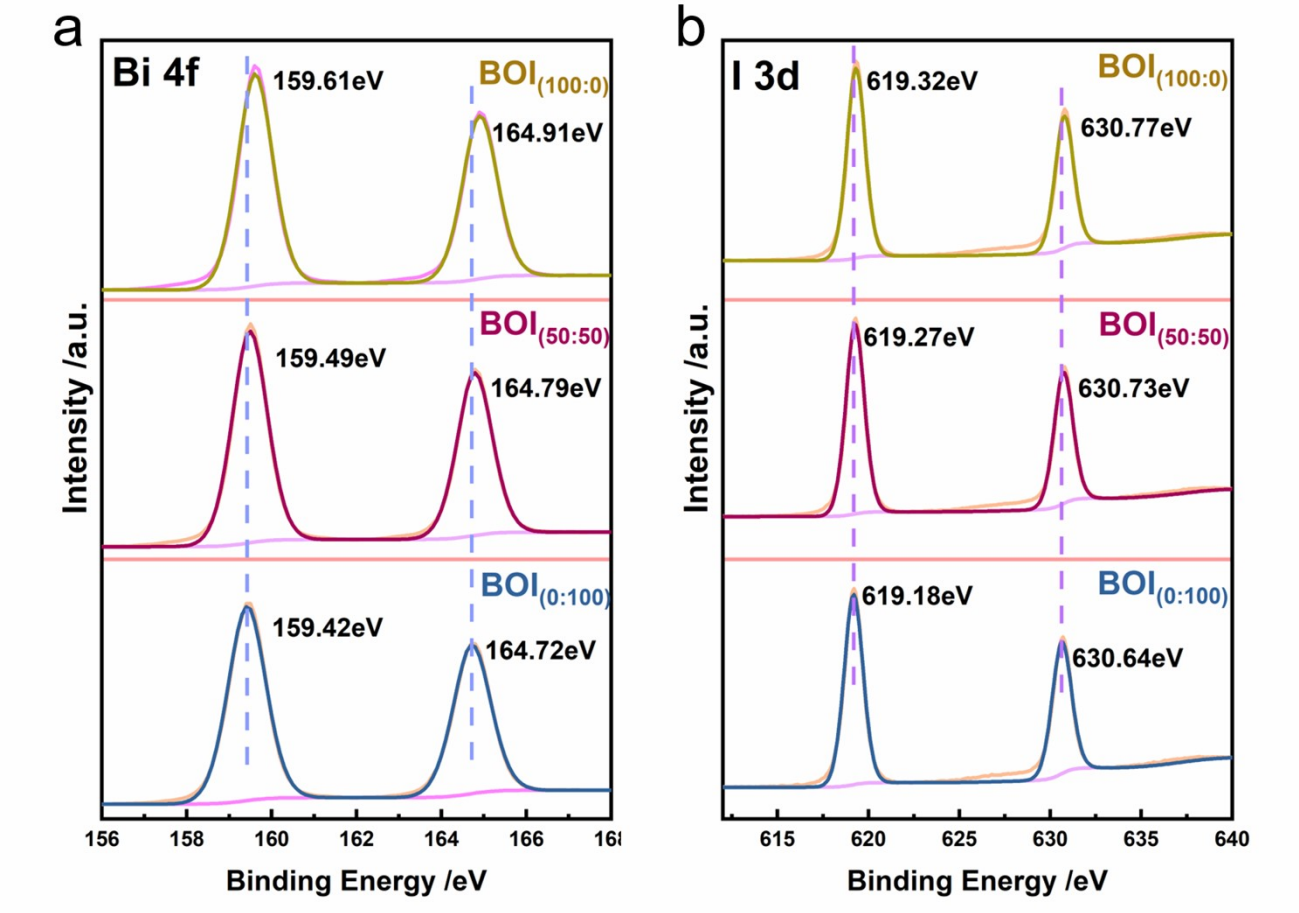

Figure S3. XPS spectra of the peaks of the Bi 4f (a), I 3d (b).

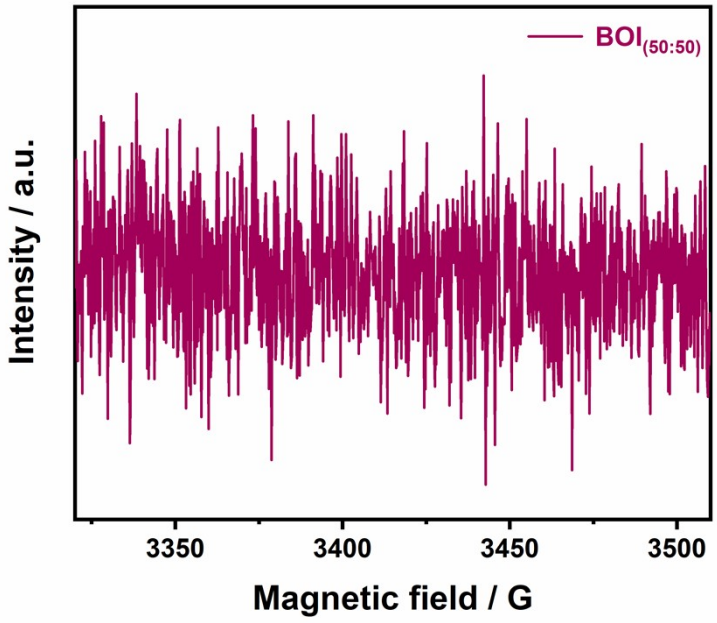

Figure S4. EPR spectra of $BOI_{(50:50)}$.

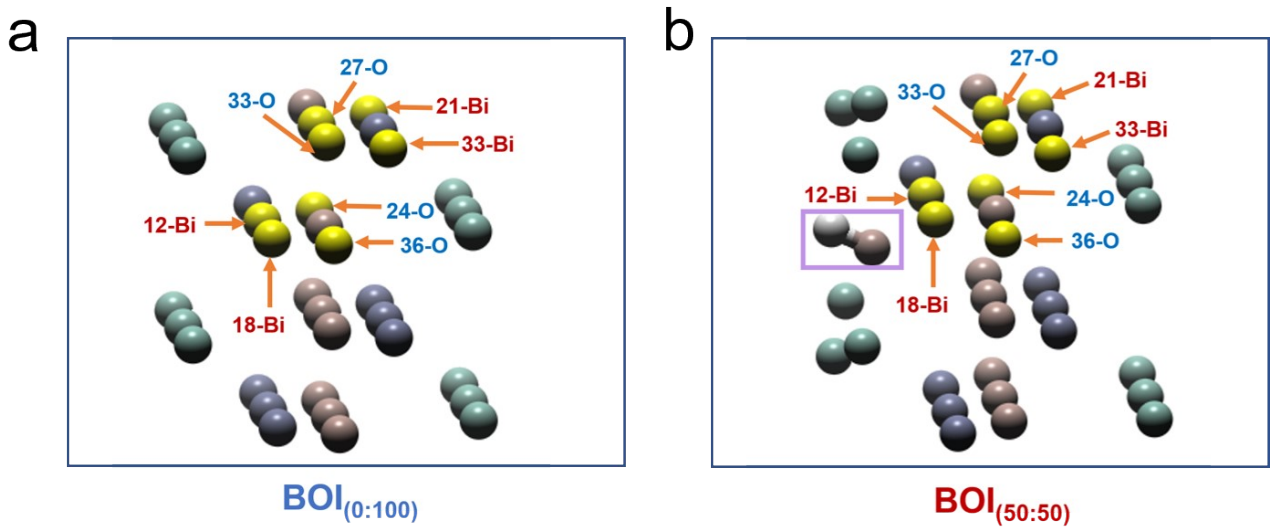

Figure S5. Selective atoms for Bi-O bonds calculation.

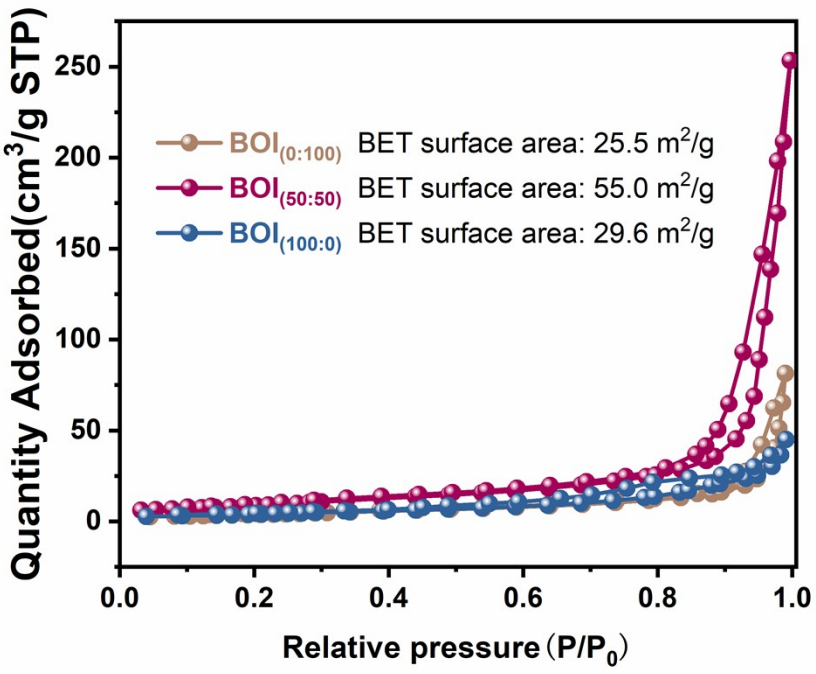

Figure S6. The specific surface area of $BOI_{(0:100)}$, $BOI_{(50:50)}$, $BOI_{(100:0)}$.

The NO_2 production was calculated from

$$\triangle = c/c_0 \times 100\% \quad \text{(S1)}$$

In this formula, c and c_0 represent the original concentration and the concentration after 30 minutes reaction of NO_2, correspondingly.

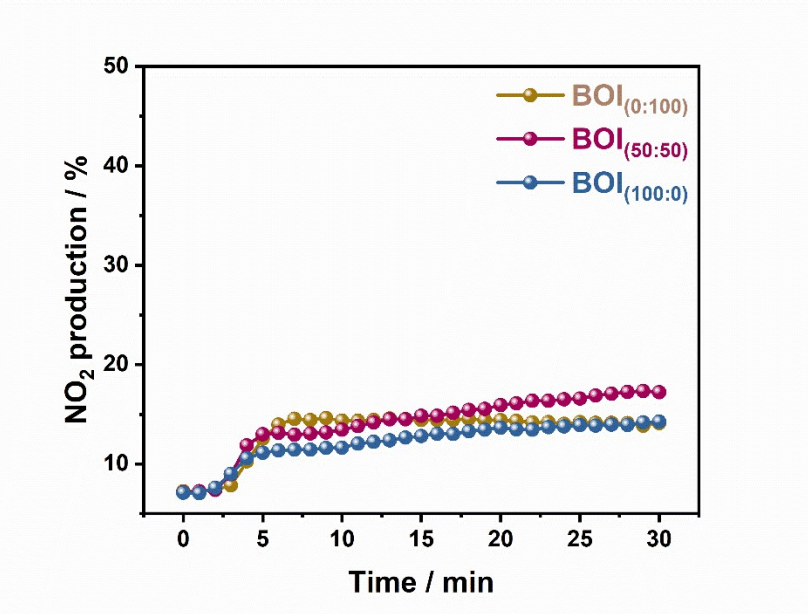

Figure S7. Photocatalytic performance of NO_2 production on $BOI_{(0:100)}$, $BOI_{(50:50)}$ and $BOI_{(100:0)}$.

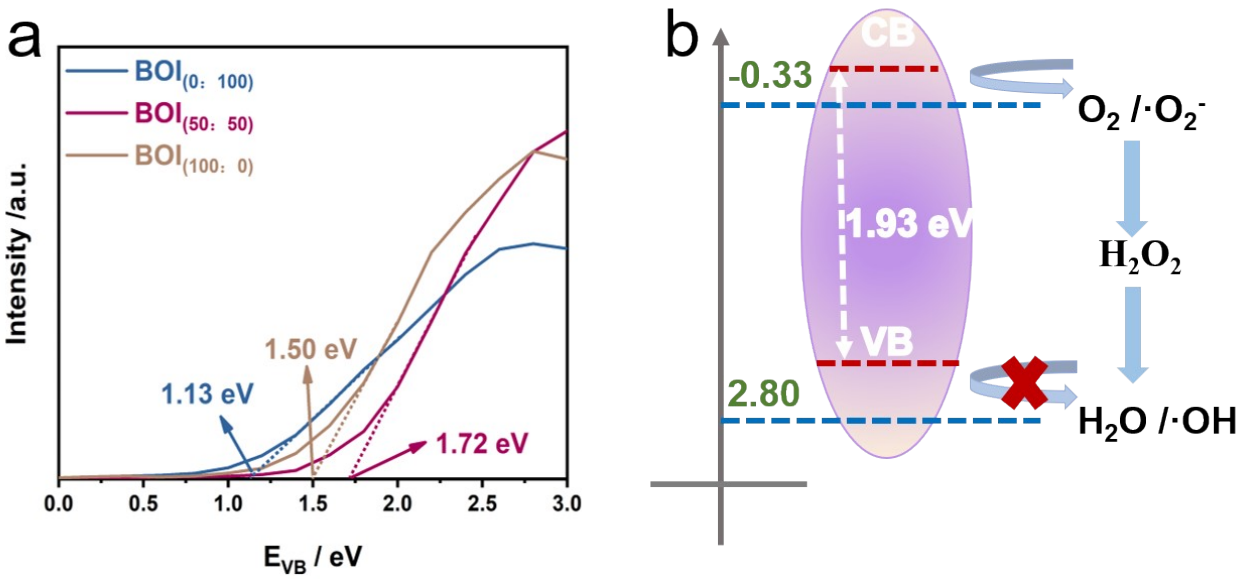

Figure S8. The proposed band structures of $BOI_{(50:50)}$ for photocatalysis mechanism.

The energy position of the valance band (E_{VB}) of $BOI_{(50:50)}$ is determined by XPS results (Figure S2 (a)) and conduction band (E_{CB}) are calculated with the following equations:

$$E_{CB} = E_{VB} - E_g \quad \text{(S2)}$$

E_g stands for the gap energy of catalysts, which can be calculated with the UV-vis results shown in Figure 3a inset.

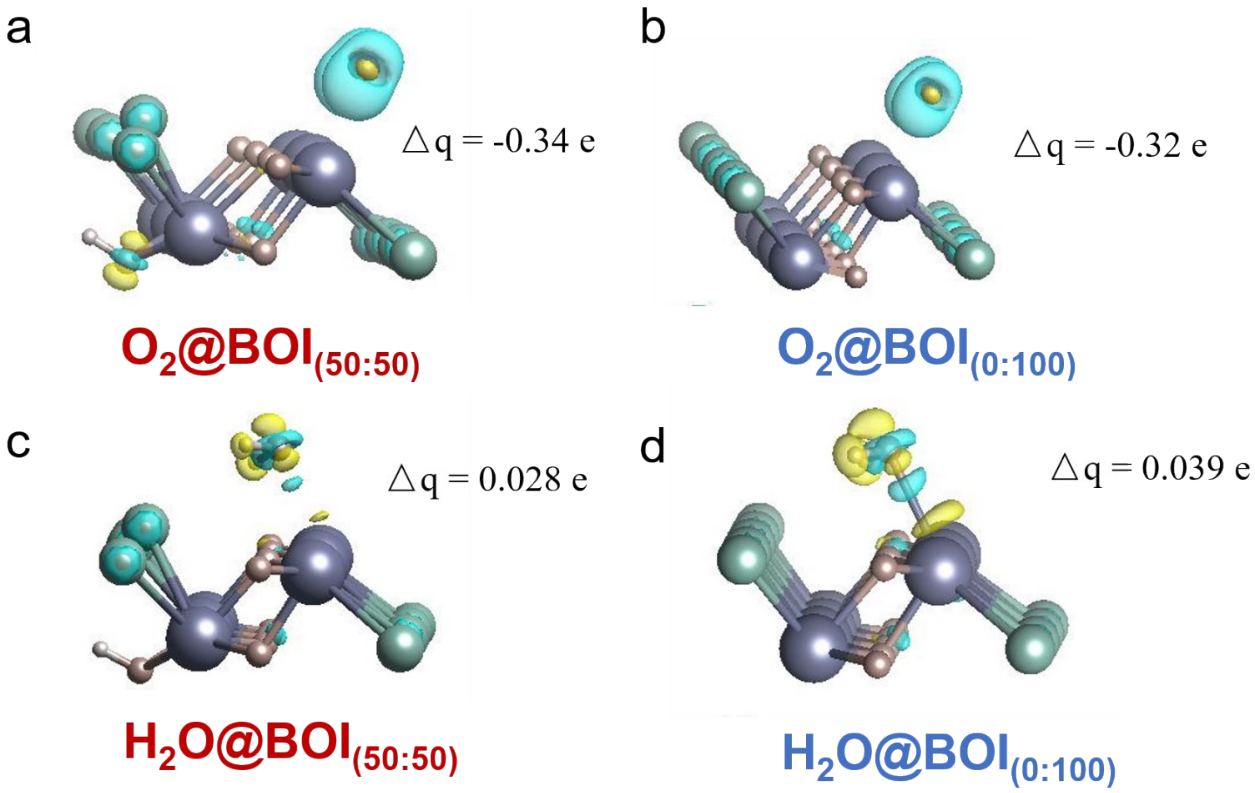

Figure S9. Electron transfer for O_2 molecules (a, b) and H_2O molecules (c, d) on BOI(50:50) and BOI(0:100): charge density difference and the Bader effective charge respectively.

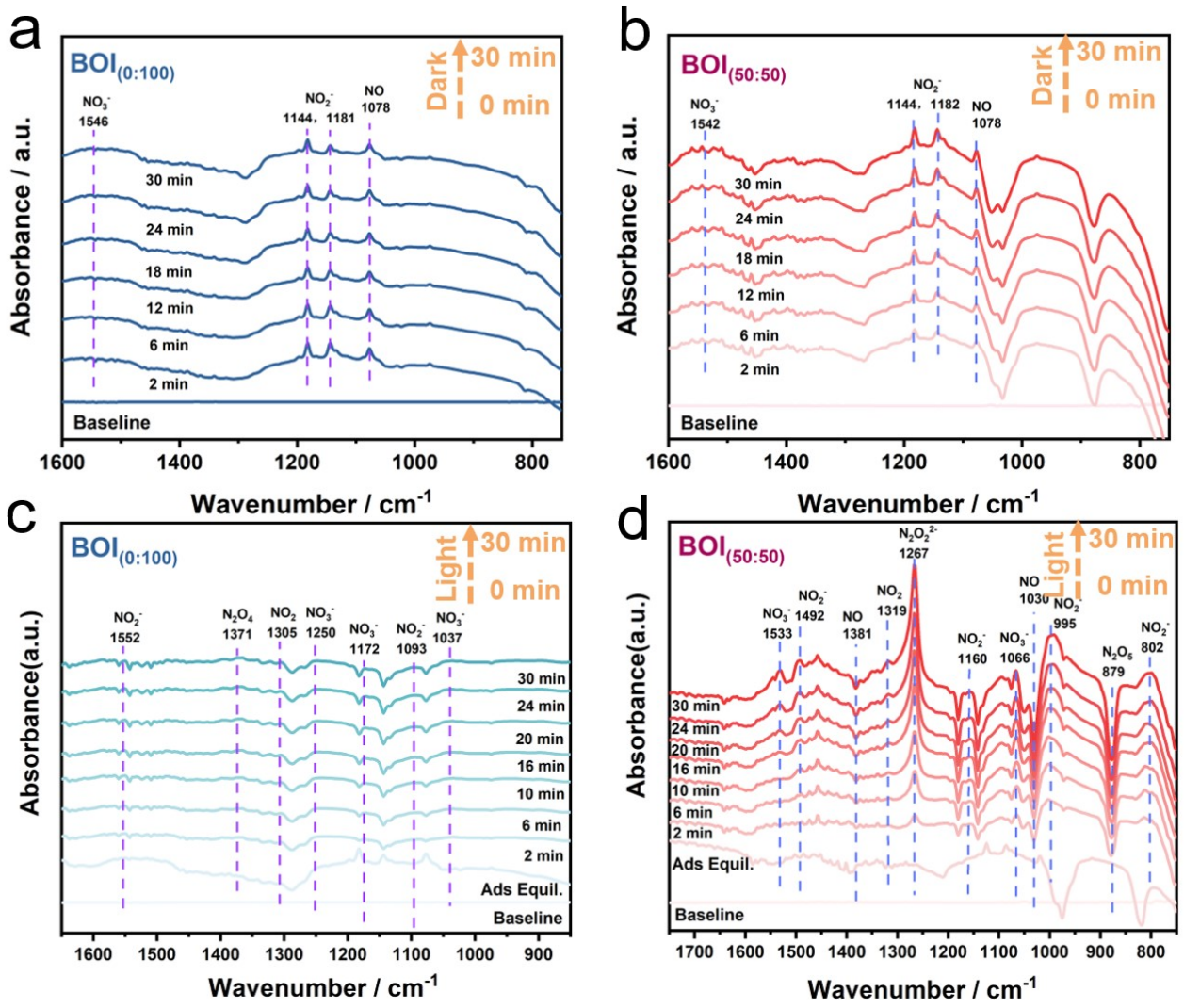

Figure S10. in situ DRIFTS spectra of NO adsorption processes over $BOI_{(0:100)}$ (a) and $BOI_{(50:50)}$ (b); Photocatalytic NO oxidation process over $BOI_{(0:100)}$ (c) and $BOI_{(50:50)}$ (d) under visible light irradiation (whole process).

Table S1. The distance of X_1 and X_2 in the three molecular diagrams after structure optimization with DFT calculation.

	$BOI_{(0,100)}$	$BOI_{(50,50)}$	$BOI_{(100,0)}$
X_1	4.607 Å	4.503 Å	4.613 Å
X_2	4.020 Å	3.967 Å	4.047 Å

Table S2. Bader charges of Bi-O bonds on BOI(0:100) sample

$BOI_{(0:100)}$				
	24-O	27-O	33-O	36-O
12-Bi	0.430 eV	0.438 eV	/	/
18-Bi	/	/	0.438 eV	0.430 eV
21-Bi	0.421 eV	0.429 eV	/	/
33-Bi	/	/	0.428 eV	0.421 eV

Table S3. Bader charges of Bi-O bonds on BOI(50:50) sample

$BOI_{(50:50)}$				
	24-O	27-O	33-O	36-O
12-Bi	0.543 eV	0.541 eV	/	/
18-Bi	/	/	0.551eV	0.557 eV
21-Bi	0.427 eV	0.424 eV	/	/
33-Bi	/	/	0.428 eV	0.429 eV

Table S4. Comparison of NO removed performance

Photocatalysts	**NO removal ratio**	**Light source**	**References**
Ba-vacancy $BaSO_4$	42.0 %	UV-light (λ = 280 nm)	[19]
Bi@OV- $Bi_2O_2CO_3$	40.8 %	Visible-light($\lambda \geq 420$ nm)	[14]
g-C_3N_4- $Bi_2O_2CO_3$	53.3 %	Visible-light($\lambda \geq 420$ nm)	[16]
Carbon vacancy-C_3N_4	47.7 %	Visible-light($\lambda \geq 448$ nm)	[54]
O/La co-functionalization in g-C_3N_4	50.4 %	Visible-light($\lambda \geq 420$nm)	[12]
BiOBr-SnO_2 heterojunctions	50.3 %	Visible-light($\lambda \geq 420$ nm)	[51]
$BaCO_3$−BiOI heterojunction	47.5%	Visible-light($\lambda \geq 420$ nm)	[33]
-OH intercalated BiOI	51.7 %	Visible-light($\lambda \geq 420$ nm)	This article

Table S5. Band assignment

Wava number (cm^{-1})	**Surface species**
1542, 1533, 1250, 1172, 1066,1037	NO_3^-
1552, 1492, 1182, 1160, 1144, 1093, 995, 802	NO_2^-
1381, 1078, 1030	NO
1371	N_2O_4
1319,1305	NO_2
1267	$N_2O_2^{2-}$
879	N_2O_5